Diagn Interv Radiol 2006; 12:17-21

ABDOMINAL IMAGING

ORIGINAL ARTICLE

Efficiency of MR imaging in the detection of malignant liver lesions

Funda Obuz, Mahmut Öksüzler, Mustafa Seçil, Özgül Sağol, Sedat Karademir, Hüseyin Astarcıoğlu

PURPOSE
To evaluate the efficacy of preoperative magnetic resonance (MR) imaging in the detection of malignant liver neoplasms.

MATERIALS AND METHODS
MR images of 23 patients who had undergone hepatic resection or liver transplantation in the last two years were evaluated retrospectively. All MR imaging studies were performed with a 1.5 T magnet using a phased-array multi-coil. The MR imaging protocol was comprised of fat-suppressed T2-weighted TSE imaging, GRE with and without fat-suppressed T1-weighted imaging, and gadolinium-enhanced multiphasic dynamic GRE imaging. Images were reviewed on a PACS workstation by two independent abdominal radiologists. The image review was conducted on a lesion-by-lesion as well as segment-by-segment basis. MR imaging findings were compared with the results of pathology studies and intraoperative ultrasound examinations. Sensitivity, specificity, and positive predictive value (PPV) of MR imaging and interobserver variation were evaluated.

RESULTS
A total of 59 malignant liver lesions in 23 patients were identified by pathology studies and intraoperative sonographic examinations. Sensitivity and PPV of MR imaging on a lesion-by-lesion analysis were 68-86% and 85-89%, respectively; kappa=0.175 and agreement was 65.8% in these analyses. Sensitivity of MR images for small (< 1cm) lesions was 13-67% and for large (> 3 cm) lesions it was 100%. In segment-by-segment analysis, sensitivity and specificity of MR images were 87-95% and 97-98%, respectively; kappa=0.207 and agreement was 76.1%. Sensitivity and PPV of MR imaging in the detection of hepatocellular carcinoma were 46-85% and 55-73%, respectively.

CONCLUSION
Although MR imaging is generally a highly accurate method for the diagnosis of malignant liver tumors, it has some difficulty in detecting small lesions and hepatocellular carcinoma in cirrhotic livers.

Key words: • *liver* • *neoplasms* • *magnetic resonance imaging*

From the Departments of Radiology (F.O. ✉ *fobuz@deu.edu.tr,* M.Ö., M.S.), Pathology (Ö.S.), and General Surgery (S.K., H.A.), Dokuz Eylül University School of Medicine, İzmir, Turkey.

Received 6 March 2005; revision requested 6 April 2005; revision received 1 September 2005; accepted 12 September 2005.

Preoperative radiological diagnosis of malignant liver lesions has recently become more important because of the increase in alternative treatment modalities for liver tumors and the expanded indications for hepatic resections in metastatic liver lesions. Cross-sectional imaging methods are usually performed for detecting the number of liver lesions and their segmental location. Magnetic resonance (MR) imaging has been performed in many studies for this aim, yet comparisons between the older technologies and MR sequences were done in those studies (1-7). The aim of the present study was to examine the efficiency of MR imaging using current standard protocols for diagnosing malignant liver lesions.

Materials and methods

Patients

We retrospectively evaluated the preoperative MR images of 23 patients who have undergone transplantation for cirrhotic livers or had undergone hepatic resection for primary or secondary malignant hepatic tumors between May 2002 and April 2004. The study group included 16 males and 7 females, with an average age of 58 years (range, 39-81 years). Ten patients had metastases of colorectal cancer, 6 had cirrhosis and/or hepatocellular carcinoma, 3 had metastases of breast cancer, 1 had metastasis of gastric cancer, 1 had peripheral cholangiocellular carcinoma, 1 had metastasis of neuroendocrine carcinoma, and 1 had hepatocellular carcinoma occurring in a non-cirrhotic liver. Twenty patients underwent hepatic resections and 3 underwent transplantations. The average time between MR imaging and surgery was 24 days (range, 3-62 days).

Technique

All patients were examined with a 1.5 T MR imaging scanner with a surface body coil. MR imaging examinations included the following sequences: TSE fat-saturated T2-weighted (TR/effective TE/ETL, 1600/70/24; 256x256 matrix; 2 NEX; slice thickness, 8 mm); GRE in-phase and out-of-phase T1-weighted (TR/TE/FA, 266/4.6-6.9/80°; 192x256 matrix; 1 NEX; slice thickness, 7 mm); post-contrast agent injection, multiphase GRE fat-saturated T1-weighted (TR/TE/FA: 136/6.9/70°; 256x256 matrix; 1 NEX) transverse images. Additionally, superparamagnetic iron oxide (SPIO) images were obtained from 9 patients.

Assessment

Two radiologists (F.O., M.S.) experienced in abdominal imaging independently conducted the radiological evaluations using PACS (picture archiving and communication system) monitors. The number, size, and segmental location of malignant liver lesions were identified using all sequences together.

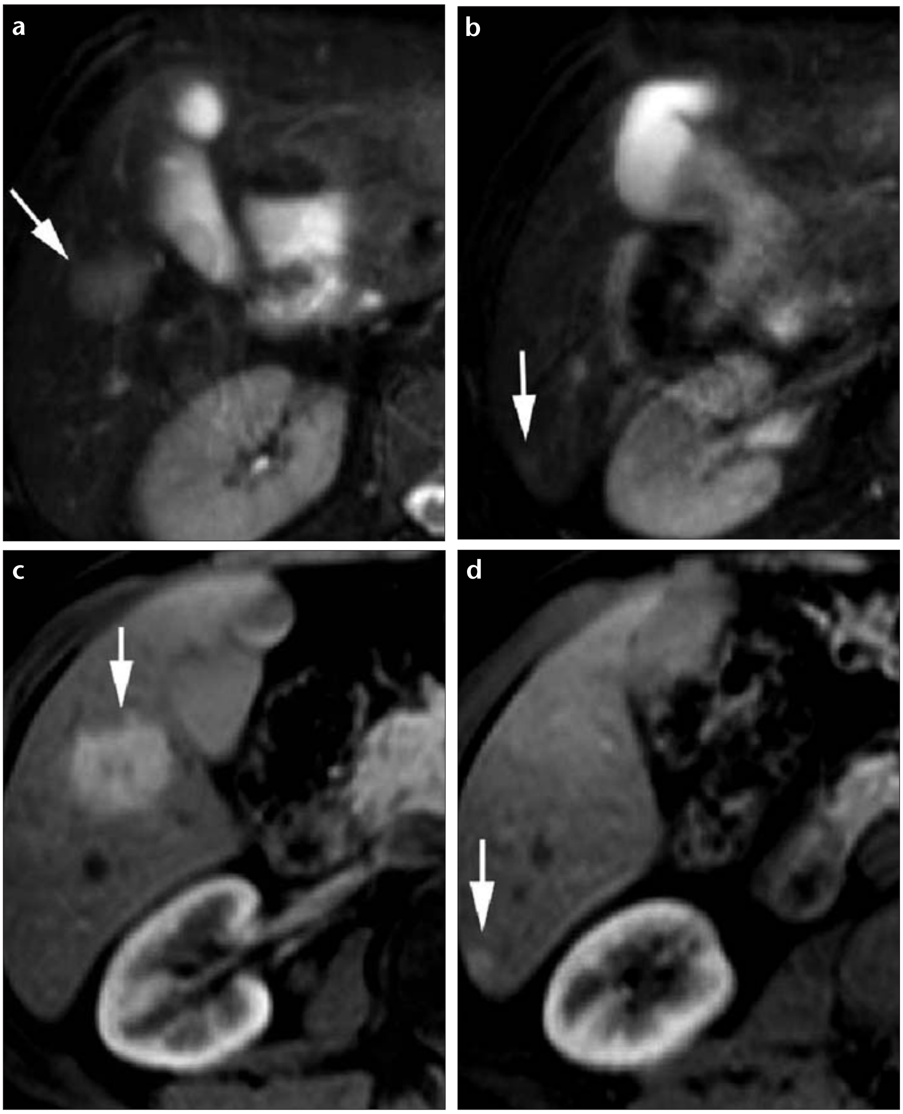

Figure 1. **a-d.** Metastases of neuroendocrine carcinoma. Transverse fat-saturated TSE T2-weighted MR images **(a, b)** show two moderately hyperintense lesions in hepatic segments 5 and 6 *(arrows)*. On transverse post-contrast fat-saturated T1-weighted images taken in the arterial phase **(c, d)**, diffuse, homogenous contrast enhancement of the lesions is seen.

Table 1. Results of the lesion-by-lesion analysis

	TP	FN	FP	Sensitivity	PPV
Observer 1[a]	51	8	6	86	89
Observer 2[a]	40	19	7	68	85

[a] Kappa: 0.175, consistency: 65.8%

TP: true positive, FN: false negative, FP: false positive, PPV: positive predictive value

Table 2. Analysis of two observers based on the size of the lesions

Lesion size	Sensitivity (Observer 1) (%)	Sensitivity (Observer 2) (%)
<1 cm	67	13
1-3 cm	93	85
>3 cm	100	100

Histopathology and intraoperative ultrasonography in 10 patients, and MR imaging follow-up (at least a 6-month interval) were accepted as the gold standard. Experienced radiologists performed intraoperative sonography with a wide-band L5-12 MHz probe.

Two kinds of evaluation were performed: lesion-by-lesion and segment-by-segment analyses. In lesion-by-lesion analysis, true positive, false positive, and false negative numbers of lesions were determined, as well as sensitivity and positive predictive value (PPV). In segment-by-segment analysis, the number of hepatic segments containing at least one lesion and containing no lesion was determined; sensitivity, specificity, and PPV and negative predictive value (NPV) were calculated. Kappa test was used for determining the correlation between the two observers.

Results

Histopathological and intraoperative US results identified a total of 59 malignant lesions in 20 of the 23 patients. There were no malignant lesions in 3 patients. Fifteen (25%) lesions were <1 cm, 40 (68%) were 1-3 cm, and 4 (7%) were >3 cm in size. Of the 59 lesions, 30 were metastases of colorectal carcinoma, 13 were hepatocellular carcinoma (HCC) (Figure 1), 6 were peripheral cholangiocellular carcinoma, 4 were metastases of gastric carcinoma, 4 were metastases of breast cancers, and 2 were metastases of neuroendocrine carcinoma (Figure 2).

The results of lesion-by-lesion analysis are shown in Tables 1 and 2. The sensitivity of MR imaging was 68-86% in lesion-by-lesion analysis; PPV was 85-89%. Kappa value was 0.175 and consistency was 65.8% in this analysis. In segment-by-segment analysis, 184 segments in 23 patients were examined. The number of segments containing at least one lesion was 39, and 145 contained no lesions. The results of segment-by-segment analysis are provided in Table 3. The sensitivity of MR imaging was 87-95% and specificity was 97-98%; kappa value was 0.207 and consistency was 76% in this analysis.

There were 8 lesions that were not detected by the evaluators. Of the 19 false negative lesions, 13 were <1 cm in size (10 metastases, 3 HCCs) and 6 were 1-3 cm (4 HCCs, 2 metastases).

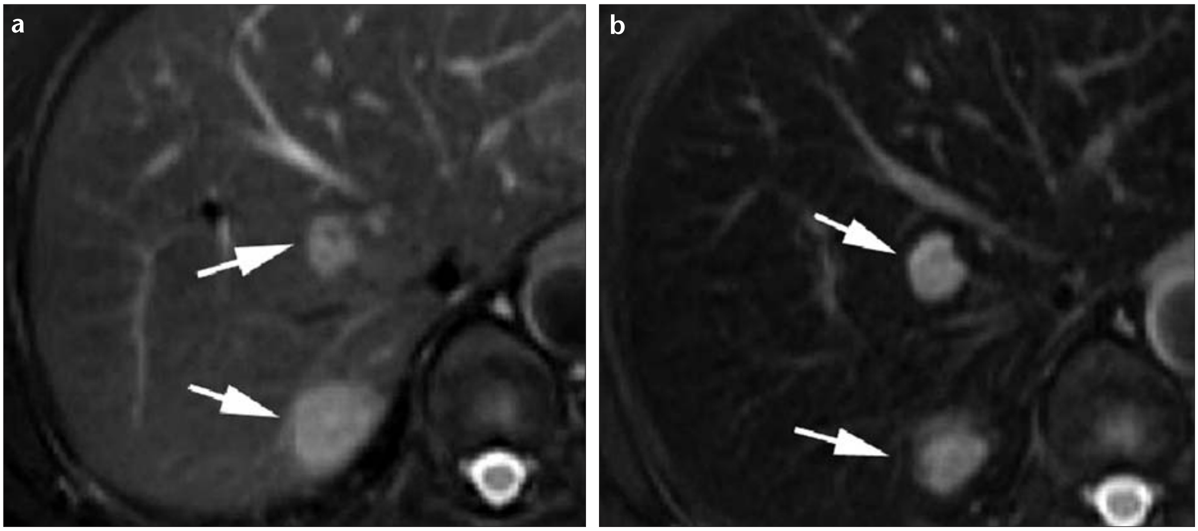

Figure 2. a, b. Metastases of breast cancer. Transverse fat-saturated TSE T2-weighted MR image **(a)** shows hyperintense metastatic nodules in hepatic segments 7 and 8. T2-weighted MR image after the administration of SPIO **(b)** reveals no difference in the number of lesions. Because the lesions did not enhance, they became more discernible from the parenchyma.

Pathological examinations revealed that, 46 of the 59 lesions were non-HCC tumors and 13 were HCCs. In determining non-HCC tumors, sensitivity of MR imaging was 74-87% and PPV was 94-95%. In determining HCCs, sensitivity was 46-85% and PPV was 55-73%.

In lesion-by-lesion analysis of the 9 patients in whom SPIO images were obtained, sensitivity of the two observers before SPIO was 81%, PPV was 81-100%; following SPIO, sensitivity was 94% and PPV was 83-100% (Figure 3).

Discussion

Determining the true number of lesions in liver tumors is very important for preoperative staging and planning of treatment. Currently, hepatic resection is in widespread use for limited metastases of colorectal, gastric, gall bladder, and breast carcinoma. Surgery or percutaneous treatment is performed in HCC due to the number of lesions and their locations. Computed tomography arterial portography (CTAP) has been the most sensitive (80-97%) method in recent years for detecting liver lesions (8-10). However, because it is invasive and has a high rate of false positivity, nowadays, other non-invasive methods are being used (7, 11, 12). Although MR imaging has high soft tissue resolution, conventional sequences have limitations in abdominal imaging. Images with high spatial and contrast resolution, and no artifacts, may be achieved by using fast T2- and T1-weighted sequences, fat saturation methods, and thin slice thickness (13). Specific and nonspecific contrast agents used in MR imaging of the liver increase accuracy (1-3, 5-7, 14, 15). It is seen that in most MR imaging studies performed for detecting lesions of the liver, sequences and contrast agents are compared to each other (3-7). In the present study, we evaluated the efficiency of MR imaging in detecting malignant liver lesions using current standard MR imaging protocol, and all sequences and dynamic imaging techniques with contrast agent together.

Table 3. Results of the segment-by-segment analysis

	Sensitivity	Specificity	Accuracy	PPV	NPV
Observer 1[a]	95	98	97	93	99
Observer 2[a]	87	97	95	87	97

[a] Kappa: 0.207, consistency: 76.1%

PPV: positive predictive value, NPV: negative predictive value

In this report, MR imaging sensitivity for small lesions (<1 cm) was 13-67%, while for large lesions (>3 cm) it was 100% for both observers. Matsuo et al. reported the sensitivity in dynamic MR imaging with contrast agent in lesions <1 cm as 55%, for lesions 1-2 cm as 85%, and for lesions >2 cm as 100% (16).

Because hepatic resection is performed according to segments, most of the lesions are detected with segment-by-segment analysis in most studies (7, 11, 12, 16). In our report, the sensitivity of MR imaging was 87-95% in the segment-by-segment analysis, which was higher than the results of lesion-by-lesion analysis (68-86%). The reason for this is that in the segment-by-segment analysis failure to observe one of the lesions in the same segment did not affect the result.

In a study that detected malignant hepatic lesions with segment-by-segment analysis, the sensitivity of MR imaging, with and without contrast agent, was 82% and the specificity was 92% (11). In the present report, the sensitivity of MR imaging with SPIO was 86% and the specificity was 95%. In another comparative study, it is reported that the sensitivity of MR imaging, with and without contrast agent, for detecting malignant lesions is higher than the imaging using SPIO (16). The superiority of dynamic MR imaging to SPIO in detecting HCC lesions in cirrhotic patients is emphasized. In cirrhotic patients, due to the

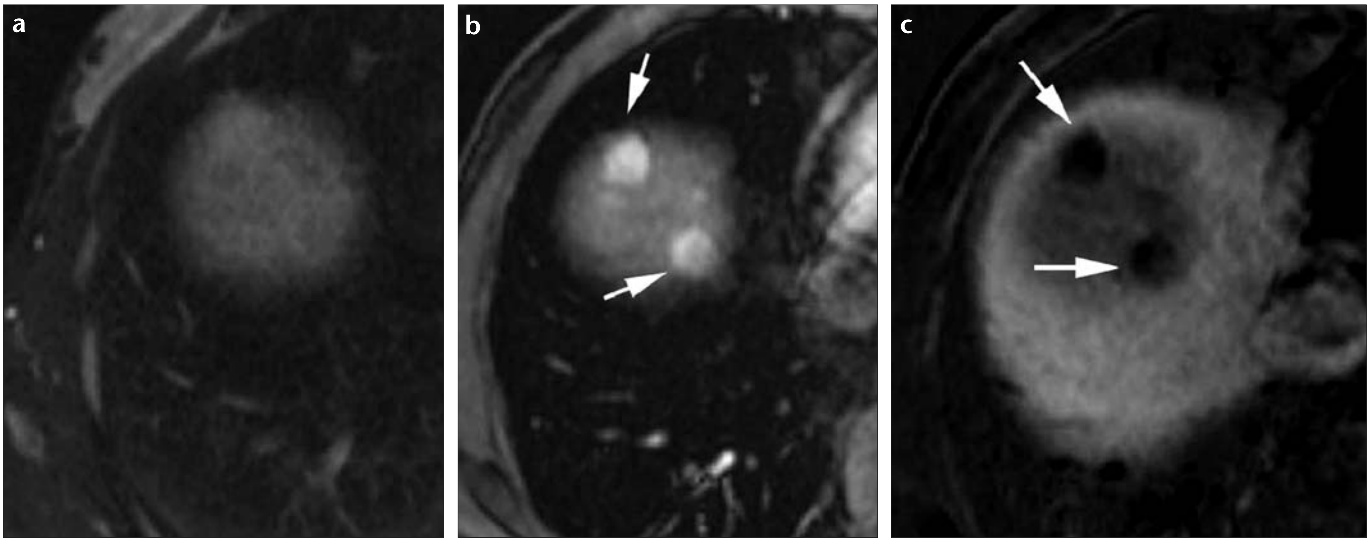

Figure 3. a-c. Hepatocellular carcinoma occurring in a cirrhotic liver. Transverse fat-saturated TSE T2-weighted MR image **(a)** shows no visible lesion. Two hyperintense lesions in the subdiaphragmatic area *(arrows)* show hypovascular nature in the arterial phase on both the T1-weighted MR image without contrast agent **(b)** and the subtraction image **(c)** performed for detecting the vascularity of these hyperintense lesions. These two lesions were diagnosed as dysplastic nodules by both radiologists.

functional liver disorder, uptake of SPIO is low and so it reduces the liver-lesion contrast difference. Additionally, well-differentiated HCCs may uptake SPIO as well (17). Kwak et al. reported that using dynamic MR imaging and SPIO together is a superior method for detecting HCCs preoperatively (12). In our study, SPIO was used in 9 patients in addition to dynamic MR imaging examination and the sensitivity was 94%. In the same 9 patients, sensitivity was 81% without using SPIO. Although this result was higher than the result of the evaluation of all the patients, 9 patients represent too small a number for statistical significance.

Krinsky et al. reported the sensitivity of dynamic MR imaging in detecting HCC lesions in cirrhotic patients who underwent transplantation as 55% (18). These results are less than the results of non-HCC lesions. This may be due to the difficulty in detecting lesions <1 cm or hypovascular lesions. Because the 3 HCC lesions in our study (1-3 cm in size) were isointense in T2-weighted sequences and hypovascular in dynamic imaging, they were accepted as dysplastic nodules. The reduced values of PPV may be explained with the high false positive ratios in this patient group. Due to parenchymal distortion and heterogeneity in cirrhotic patients, gross fibrotic foci may be detected as HCC. Moreover, due to hypervascularity, parenchymal arterioportal shunts, and some dysplastic nodules may not be distinguishable from HCC (12, 18).

One of the limitations of our study is that because it was retrospective the time period between MR imaging and surgery was long. This may have caused errors, especially in detecting small lesions. Although the images were evaluated by two radiologists who are experienced in abdominal imaging, the correlation between each of their evaluations was low (kappa, 0.175 and 0.207). As the identities of the patients, and surgical and pathological information were kept confidential, the cause of the low correlation between the two observers may have been due to differences in their experience. As exemplified in the literature, the observers may be chosen from outside the clinic for reducing the bias.

In conclusion, MR imaging is highly accurate in detecting malignant liver lesions, although it has some difficulty in detecting small lesions, especially <1 cm, and HCC in cirrhotic patients.

References

1. Low RN, Francis IR, Herfkens RJ, et al. Fast multiplanar spoiled gradient-recalled imaging of the liver: pulse sequence optimization and comparison with spin-echo MR imaging. AJR Am J Roentgenol 1993; 160:501-509.
2. Yamashita Y, Hatanaka Y, Yamamato H, et al. Differential diagnosis of focal liver lesions: role of spin-echo and contrast-enhanced dynamic MR imaging. Radiology 1994; 193:59-65.
3. Larson RE, Semelka RC, Bagley AS, Molina PL, Brown ED, Lee JK. Hypervascular malignant liver lesions: comparison of various MR imaging pulse sequences and dynamic CT. Radiology 1994; 192:393-399.
4. Kanematsu M, Hoshi H, Murakami T, et al. Focal hepatic lesion detection: comparison of four T2-weighted MR imaging pulse sequences. Radiology 1998; 206:167-175.
5. Dromain C, Baere T, Baudin E, et al. MR imaging of hepatic metastases caused by neuroendocrine tumors: comparing four techniques. AJR Am J Roentgenol 2003; 180:121-128.
6. del Frate CD, Bazzocchi M, Mortele KJ, et al. Detection of liver metastases: comparison of gadobenate dimeglumine-enhanced and ferumoxides-enhanced MR imaging examinations. Radiology 2002; 225:766-772.
7. Vogl TJ, Schwarz W, Blume S, et al. Preoperative evaluation of malignant liver tumors: comparison of unenhanced and SPIO (Resovist)-enhanced MR imaging with biphasic CTAP and introperative US. Eur Radiol 2003; 13:262-272.
8. Heiken JP, Weyman PJ, Lee JK, Balfe DM, Picus D, Brunt EM, Fyle MW. Detection of focal hepatic masses: prospective evaluation with CT, delayed CT, CT during arterial portography, and MR imaging. Radiology 1989; 171:47-51.
9. Matsui O, Takashima T, Kadoya M, et al. Dynamic computed tomography during arterial portography: the most sensitive examinations for small hepatocellular carcinomas. J Comput Assist Tomogr 1985; 9:19-24.
10. Nelson RC, Chezmar JL, Sugarbaker PH, Bernardino ME. Hepatic tumors: comparison of CT during arterial portography, delayed CT, and MR imaging for preoperative evaluation. Radiology 1989; 172:27-34.

11. Kondo H, Kanematsu M, Hoshi H, et al. Preoperative detection of malignant hepatic tumors: comparison of combined methods of MR imaging with combined methods of CT. AJR Am J Roentgenol 2000; 174:947-954.
12. Kwak HS, Lee JM, Kim CS. Preoperative detection of hepatocellular carcinoma: comparison of combined contrast-enhanced MR imaging and combined CT during arterial portography and CT hepatic arteriography. Eur Radiol 2004; 14:447-457.
13. Semelka RC, Cance WG, Marcos HB, Mauro MA. Liver metastases: comparison of current MR techniques and spiral CT during arterial portography for detection of 20 sugically staged cases. Radiology 1999; 213:86-91.
14. Ros PR, Freeny PC, Harms SE, et al. Hepatic MR imaging with ferumoxides: a multicenter clinical trial of the safety and efficacy in the detection of focal hepatic lesions. Radiology 1995; 196:481-488.
15. Reimer P, Jahnke N, Fiebich M, et al. Hepatic lesion detection and characterization: value of nonenhanced MR imaging, superparamagnetic iron oxide-enhanced MR imaging, and spiral CT–ROC analysis. Radiology 2000; 217:152-158.
16. Matsuo M, Kanematsu M, Itoh K, et al. Detection of malignant hepatic tumors: comparison of gadolinium- and ferumoxide-enhanced MR imaging. AJR Am J Roentgenol 2001; 177:637-643.
17. Ward J, Guthrie JA, Scott DJ. Hepatocellular carcinoma in the cirrhotic liver: double MR contrast imaging for diagnosis. Radiology 2000; 216:154-162.
18. Krinsky GA, Lee VS, Theise ND, Weinreb JC, Rofsky NM, Diflo T, Teperman LW. Hepatocellular carcinoma and dysplatic nodules in pattients with cirrhosis: prospective diagnosis with MR imaging and explantation corelation. Radiology 2001; 219:445-454.